C. R. Physique 15 (2014) 393–402

Contents lists available at ScienceDirect

Comptes Rendus Physique

www.sciencedirect.com

Electromagnetism / Électromagnétisme

An implicit FDTD scheme for the propagation of VLF–LF radio waves in the Earth–ionosphere waveguide

Un schéma FDTD implicite pour la propagation radio VLF–LF dans le guide d'onde Terre–ionosphère

Jean-Pierre Bérenger

JPB Consultant, 5, rue des Docteurs Thiers, 26400 Crest, France

ARTICLE INFO

Article history:
Available online 2 June 2014

Keywords:
Communication
Propagation
VLF
LF
FDTD

Mots-clés :
Communication
Propagation
VLF
LF
FDTD

ABSTRACT

A new finite-difference time-domain scheme is presented for the propagation of VLF–LF radio waves in the Earth–ionosphere waveguide. The new scheme relies on the implicit solution of the auxiliary equation that governs the current density in the ionosphere. The advantages and drawbacks of the new scheme are discussed. Its main advantage is its stability condition, which is the same as that of the FDTD method in a vacuum. This permits the time step of the calculation to be increased and then the overall computational time to be reduced. Numerical experiments demonstrate the accuracy of the new scheme and the reduction of the computational time.

RÉSUMÉ

Cet article décrit un nouveau schéma aux différences finies pour la propagation VLF–LF dans le guide d'onde Terre–ionosphère. Ce schéma repose sur une solution implicite de l'équation auxiliaire qui gouverne la densité de courant dans l'ionosphère. Les avantages et inconvénients du nouveau schéma sont discutés. Son principal avantage tient dans sa condition de stabilité qui est identique à celle de la méthode FDTD dans le vide. Cela permet d'augmenter le pas temporel de la résolution FDTD et, en conséquence, de réduire le temps de calcul. Des résultats de calcul illustrent la bonne précision du nouveau schéma et les réductions de temps calcul qu'il permet d'obtenir.

1. Introduction

Very low-frequency (VLF) and low-frequency (LF) waves can propagate within the Earth–ionosphere waveguide, providing reliable communication links over thousands of kilometers. Before the introduction of the GPS system, the VLF band has been used for several decades for radionavigation purposes. Nowadays, the 10–70-kHz frequency band remains used to transmit toward submarines, because such frequencies can be received a few meters under the sea surface. To predict the propagation of VLF–LF waves, two numerical methods were developed during the years 1960–1980 [1–3]. The most used is the waveguide method, which relies on a modal development of the field within the waveguiding structure. The

http://dx.doi.org/10.1016/j.crhy.2014.05.002
1631-0705/

second method, known as the wavehop method, is a ray method. Both methods were well suited to the computers of the 1960–1980 years because they are effective in terms of computational cost. However, they have some drawbacks. Mainly, they cannot take into account continuous variations of the radiopath, which must be composed of segments where the ionosphere and the ground are uniform.

During the years 1990–2000 [4–7], a third method was introduced for VLF–LF calculations, the finite-difference time-domain (FDTD) method [8]. The motivations of these works were mainly the validation of the previous techniques and the possibility of taking into consideration any variations of the physical parameters along the radiopath.

With the scheme in [5,6], the Maxwell equations are solved with the FDTD method in parallel with the differential equation that connects the electric field to the electronic current in the ionosphere. This scheme yields accurate results, as demonstrated by numerous comparisons with the waveguide technique. The price of the full-wave FDTD method is a far larger computational time, but this is a drawback increasingly small as the computers become increasingly powerful.

After developing a computer code based on [5,6], several papers appeared on FDTD schemes in the ionosphere [9–12]. Although they addressed other applications, they appeared of potential interest for the VLF–LF propagation. The most interesting idea is the use of an implicit scheme in place of the full explicit scheme [6] for solving the auxiliary equation that governs the current density in the medium. Introduced in [9] in non-magnetized plasmas, it was later used in the magnetized ionosphere [11,12]. With such a scheme, the advances of the electric field and the current density at each FDTD node are no longer explicit; they depend on each other and form a set of equations that must be solved at each time step. This is a drawback, but the implicit scheme has a major interest, its stability condition, which is the same as in a vacuum, conversely to that of scheme [6], which is more severe. For this reason, investigations have been performed in recent years on the application of an implicit scheme to the VLF–LF propagation. Starting from [6] and using the ideas in [9], a new scheme has been developed. It is more compact and effective than the one in [12], later extended to three dimensions in [13]. It permits significant reductions of the computational time in comparison with the scheme [6], and renders the FDTD time step independent of the physical parameters of the ionosphere, which is a highly desirable feature.

This paper briefly presents the application of the FDTD method to VLF–LF propagation and summarizes the explicit scheme [6]. It describes with details the new implicit scheme, discusses the advantages and drawbacks of the two schemes, and shows various numerical experiments that validate the new scheme and illustrate its effectiveness in VLF–LF calculations.

2. The ionospheric medium

There are several species in the ionosphere, the electrons, the positive ions, and the negative ions [1]. When an electromagnetic wave propagates in the medium, current densities of electrons and ions are produced. Except in special conditions, the effect of the ions on the propagation of VLF–LF waves in the Earth–ionosphere waveguide is negligible [1]. The equation that connects the electric field E to the current density of electrons J can be obtained by equating to zero the sum of the forces applied to the electrons, namely the inertia force, the Coulomb force, the Lorentz force due to the natural magnetic field, and the friction force due to collisions with neutrals. This yields [1,6]:

$$\frac{\mathrm{d}\vec{J}}{\mathrm{d}t} + \frac{e}{m}\vec{J} \wedge \vec{B}_0 + \nu\vec{J} = \varepsilon_0\omega_\mathrm{p}^2\vec{E} \tag{1}$$

with:

$$\omega_\mathrm{p}^2 = \frac{Ne^2}{m\varepsilon_0} \tag{2}$$

where e and m are the charge and the mass of one electron, B_0 is the natural magnetic field, N is the electronic density, and ν is the electron–neutral collision frequency. Quantity ω_p is called the plasma frequency.

Using the FDTD method to compute the propagation of VLF–LF waves in the ionosphere consists in solving in parallel Eq. (1) with the Maxwell equations:

$$\varepsilon_0\frac{\partial\vec{E}}{\partial t} + \vec{J} = \vec{\nabla} \times \vec{H} \tag{3}$$

$$\mu_0\frac{\partial\vec{H}}{\partial t} = -\vec{\nabla} \times \vec{E} \tag{4}$$

3. The FDTD method for the VLF–LF propagation

As with other numerical techniques [1–3], the VLF–LF propagation is assumed as symmetric with respect to the radiopath, so that the computational domain is a two-dimensional (2D) domain that holds the transmitter and the radiopath. The plane where the FDTD domain is lying is represented in Fig. 1. The problem is solved in spherical coordinates. The 2D Maxwell equations are obtained by using the symmetry, i.e. by equating to zero the derivatives in φ direction in the general 3D equations. FDTD discretization in spherical coordinates can be found in [6,8].

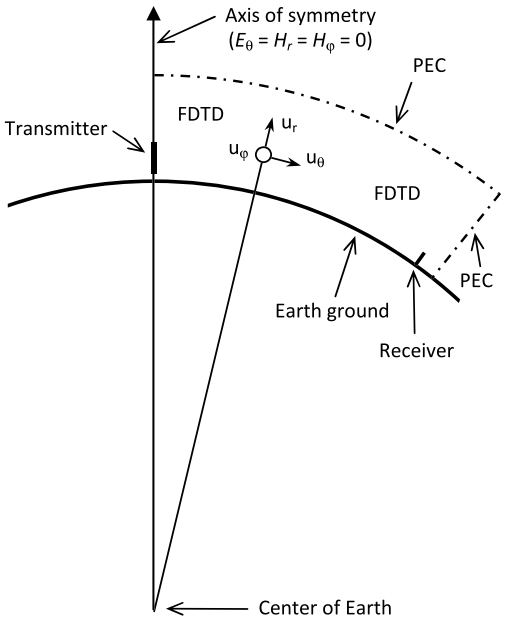

Fig. 1. The 2D VLF–LF problem in spherical coordinates. The region between the axis of symmetry, the Earth surface, and the dashed line (PEC) is the FDTD computational domain.

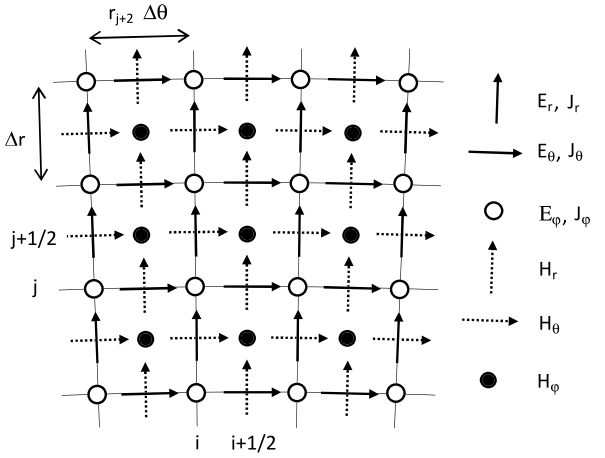

Fig. 2. The FDTD mesh.

The Maxwell equations are solved between the Earth surface and an altitude of the order of 100 km. The transmitter is placed to the left, upon the vertical axis of symmetry where $E_\theta = H_r = H_\varphi = 0$. The radiated field propagates in the whole domain, up to the end of the radiopath (called receiver). The top of the domain is placed above the altitude of reflection of the waves so that a perfect electric condition (PEC) can be applied to it. A PEC is also applied to the right-hand-side boundary, placed far enough so that the artificial reflection it produces is not viewed at the receiver's location.

The FDTD domain is discretized with FDTD cells. The components E_r, E_θ, E_φ, H_r, H_θ, H_φ, are computed at the nodes of the grid in Fig. 2. The components of the current density, J_r, J_θ, J_φ, are computed at the same nodes as E_r, E_θ, E_φ.

The ground is on a line E_θ, E_φ, H_r. It may be either a perfect conductor ($E_\theta = E_\varphi = H_r = 0$), or a lossy medium (seawater, any soil). In the latter case, the ground is taken into account by the surface impedance method [7]. The transmitter radiates a sinusoidal wave. Its magnitude and phase are recorded at the points of interest after a brief transient state. To reduce the computational time, the actual FDTD domain is a moving domain a few hundred kilometers in length that follows the sinusoidal pulse as it propagates throughout the waveguide (see more details in [7]).

With the FDTD method, E and H are computed at times separated with half a time step, usually denoted as n and $n + 1/2$. When a current density J is present, it is discretized at the same times as H [8]. This is true with the explicit scheme [6], but will not be true with the implicit scheme with which J will be computed at the same times as E. The discretization of Eq. (1), called an auxiliary equation in the FDTD context, is addressed with details in the next section.

4. Discretization of the auxiliary equation

4.1. The explicit scheme

With scheme [6], the current density is computed at times $n+1/2$, while the electric field is computed at times n. From this, using (3) the FDTD advance of the E vector from time n to time $n+1$ can be written in compact form as:

$$\vec{E}^{n+1} = \vec{E}^{n} - \frac{\Delta t}{\varepsilon_0}\vec{J}^{n+1/2} + \frac{\Delta t}{\varepsilon_0}\vec{\nabla}\times\vec{H}^{n+1/2} \tag{5}$$

where it is understood that components E_r, E_θ, E_φ are computed at their own nodes of the staggered FDTD grid (Fig. 2).

The auxiliary equation (1) is used to advance the current density components which are collocated in space with the E components. Consider for instance the r component of (1). It reads:

$$\frac{\partial J_r}{\partial t} + \nu J_r + \frac{e}{m}B_\varphi J_\theta - \frac{e}{m}B_\theta J_\varphi = \varepsilon_0\omega_p^2 E_r \tag{6}$$

where B_θ, B_φ are components of the natural field B_0. It is well known that such an equation, where the function to be advanced and its derivative on time are present, can be linearly discretized only for small enough time steps, here on condition that $\nu\Delta t \ll 1$. The condition does not hold with ν and Δt values of interest in the VLF–LF propagation problem, so that the equation must be considered as a first-order differential equation that governs J_r for the time step Δt. Here, an additional difficulty is the presence of the other two components in the equation, J_θ and J_φ. Similarly, the three components also are present in the θ and φ components of (1), which are similar to (6). The three equations are not independent; they form a system of three first-order differential equations for the three unknown functions J_r, J_θ, J_φ. In [6], the problem has been simplified by replacing the J_θ and J_φ functions in (6) with the average of their values at the beginning and at the end of the considered time step. This permits the three differential equations to be independent. Explicitly, Eq. (6) is rewritten as:

$$\frac{\partial J_r}{\partial t} + \nu J_r + \frac{e}{m}B_\varphi\frac{J_\theta^{n-1/2}+J_\theta^{n+1/2}}{2} - \frac{e}{m}B_\theta\frac{J_\varphi^{n-1/2}+J_\varphi^{n+1/2}}{2} = \varepsilon_0\omega_p^2 E_r^n \tag{7}$$

which governs J_r from $n-1/2$ to $n+1/2$. Solving this differential equation for J_r, the following differencing is obtained:

$$J_r^{n+1/2} = a J_r^{n-1/2} + b\left[-\omega_{b\varphi}\frac{J_\theta^{n-1/2}+J_\theta^{n+1/2}}{2} + \omega_{b\theta}\frac{J_\varphi^{n-1/2}+J_\varphi^{n+1/2}}{2} + \varepsilon_0\omega_p^2 E_r^n\right] \tag{8}$$

where:

$$a = e^{-\nu\Delta t} \qquad b = \frac{1-e^{-\nu\Delta t}}{\nu} \tag{9}$$

$$\omega_{br} = \frac{e}{m}B_r \qquad \omega_{b\theta} = \frac{e}{m}B_\theta \qquad \omega_{b\varphi} = \frac{e}{m}B_\varphi \tag{10}$$

Proceeding similarly with the other two components of (1), the following is obtained:

$$A\vec{J}^{n+1/2} = B\vec{J}^{n-1/2} + b\varepsilon_0\omega_p^2\vec{E}^n \tag{11}$$

where:

$$A = \begin{pmatrix} 1 & \frac{b\omega_{b\varphi}}{2} & -\frac{b\omega_{b\theta}}{2} \\ -\frac{b\omega_{b\varphi}}{2} & 1 & \frac{b\omega_{br}}{2} \\ \frac{b\omega_{b\theta}}{2} & -\frac{b\omega_{br}}{2} & 1 \end{pmatrix} \qquad B = \begin{pmatrix} a & -\frac{b\omega_{b\varphi}}{2} & \frac{b\omega_{b\theta}}{2} \\ \frac{b\omega_{b\varphi}}{2} & a & -\frac{b\omega_{br}}{2} \\ -\frac{b\omega_{b\theta}}{2} & \frac{b\omega_{br}}{2} & a \end{pmatrix} \tag{12}$$

Eq. (11) can be rewritten in the form:

$$\vec{J}^{n+1/2} = M_1\vec{J}^{n-1/2} + b\varepsilon_0\omega_p^2 M_2\vec{E}^n \tag{13}$$

with:

$$M_1 = A^{-1}B \qquad M_2 = A^{-1} \tag{14}$$

Assuming that E is known at time n, Eq. (13) permits J to be explicitly advanced from $n-1/2$ to $n+1/2$, in parallel with the advance of H.

It was demonstrated [6] that the above differencing, called a semi-exponential differencing, yields accurate results in the VLF–LF propagation problem. However, a rigorous exponential differencing can be derived because of the existence of an

analytical solution for the system of three coupled differential equations formed with (6) and the other two components of (1). This solution was published in [10]. We have derived the corresponding exponential differencing. The advance of J is in the same form as (13), with just two matrices that differ from M_1 and M_2. Numerical experiments have been performed to compare the two differencings. They yield superimposed results in most cases. However, in some cases, the calculation with the true exponential differencing is instable. The reason may be the presence of trigonometric functions in the analytical solution of the ionospheric system [10], which may render the matrices singular in some cases.

The stability condition is a critical parameter in FDTD schemes. In 2D Cartesian coordinates, the Yee FDTD scheme is stable in a vacuum provided that the time step Δt satisfies the CFL condition [8]:

$$\Delta t < \frac{1}{c}\frac{1}{\sqrt{\frac{1}{\Delta x^2}+\frac{1}{\Delta y^2}}} \tag{15}$$

where Δx and Δy are the space steps. In the VLF–LF spherical coordinates, the condition is approximately valid with $\Delta x = r_{\text{Earth}}\Delta\theta$ and $\Delta y = \Delta r$. In the case of the explicit scheme, the stability condition was derived in [6] in the absence of natural magnetic field (isotropic case). It reads:

$$\Delta t < \frac{1}{c}\frac{1}{\sqrt{\frac{1}{\Delta x^2}+\frac{1}{\Delta y^2}+\frac{\omega_p^2}{4c^2}}} \tag{16}$$

It was observed that this condition also ensures stability with the natural B field. Because of the additional term in the denominator, the condition is more severe than in a vacuum. It depends on the electronic density through ω_p. The difference with a vacuum depends on the space steps of the calculation and on the maximum electronic density in the computational domain. In actual calculations of VLF–LF propagation, the time step is reduced by a factor which may be about 3 or 4 in some cases, mainly at low frequencies, where space steps are large. This is a serious drawback of the explicit scheme.

4.2. The implicit scheme

Another discretization of the auxiliary equation (1) was discussed in [9] for non-magnetized plasmas ($B_0 = 0$). It consists in computing the current J at the same times as the electric field E, that is at times n in place of times $n+1/2$. Starting from this idea, an implicit scheme is derived in the following for the VLF–LF propagation in the ionosphere. Assuming that J is computed at times n, the differencing of (3) reads, in place of (5):

$$\vec{E}^{n+1} = \vec{E}^{n} - \frac{\Delta t}{\varepsilon_0}\frac{\vec{J}^{n}+\vec{J}^{n+1}}{2} + \frac{\Delta t}{\varepsilon_0}\vec{\nabla}\times\vec{H}^{n+1/2} \tag{17}$$

and for the advance of J_r from time n to time $n+1$, (7) is replaced with:

$$\frac{\partial J_r}{\partial t} + \nu J_r + \frac{e}{m}B_\varphi\frac{J_\theta^n + J_\theta^{n+1}}{2} - \frac{e}{m}B_\theta\frac{J_\varphi^n + J_\varphi^{n+1}}{2} = \varepsilon_0\omega_p^2\frac{E_r^n + E_r^{n+1}}{2} \tag{18}$$

which yields the semi-exponential differencing (8) shifted with $\Delta t/2$ and with the averaged electric field in the right-hand member. Doing the same for the other two components of (1), the following advance of J vector is obtained:

$$A\vec{J}^{n+1} = B\vec{J}^{n} + b\varepsilon_0\omega_p^2\frac{\vec{E}^{n}+\vec{E}^{n+1}}{2} \tag{19}$$

where matrices A and B remain given by (12). At the end, the following is obtained, in place of (13):

$$\vec{J}^{n+1} = M_1\vec{J}^{n} + b\varepsilon_0\omega_p^2 M_2\frac{\vec{E}^{n}+\vec{E}^{n+1}}{2} \tag{20}$$

As they stand, Eqs. (17) and (20) do not permit the explicit advance of E and J from time n to time $n+1$. They form a set of two equations for the two unknown vectors E and J at time $n+1$. Combining the two equations, explicit formulae can be obtained. Using for instance (20) into (17) yields:

$$\vec{E}^{n+1} = \vec{E}^{n} - \frac{\Delta t}{2\varepsilon_0}\vec{J}^{n} - \frac{\Delta t}{2\varepsilon_0}M_1\vec{J}^{n} - \frac{\Delta t}{2\varepsilon_0}\frac{b\varepsilon_0\omega_p^2}{2}M_2\vec{E}^{n} - \frac{\Delta t}{2\varepsilon_0}\frac{b\varepsilon_0\omega_p^2}{2}M_2\vec{E}^{n+1} + \frac{\Delta t}{\varepsilon_0}\vec{\nabla}\times\vec{H}^{n+1/2}$$

from which the following explicit formula is obtained for E^{n+1}:

$$\vec{E}^{n+1} = M_3\vec{E}^{n} - \frac{\Delta t}{2\varepsilon_0}M_4\vec{J}^{n} + \frac{\Delta t}{\varepsilon_0}M_5\vec{\nabla}\times\vec{H}^{n+1/2} \tag{21}$$

where, using (14):

$$M_3 = [I + \theta M_2]^{-1}[I - \theta M_2] = \left[I + \theta A^{-1}\right]^{-1}\left[I - \theta A^{-1}\right] \tag{22}$$

$$M_4 = [I + \theta M_2]^{-1}[I + M_1] = \left[I + \theta A^{-1}\right]^{-1}\left[I + A^{-1}B\right] \tag{23}$$

$$M_5 = [I + \theta M_2]^{-1} = \left[I + \theta A^{-1}\right]^{-1} \tag{24}$$

$$\theta = \frac{b\Delta t\omega_p^2}{4} \tag{25}$$

By advancing first the E field with (21), the current can be advanced using (20).

An explicit current can also be derived from (17) and (20). Using (17) into (20) yields:

$$\vec{J}^{n+1} = M_1\vec{J}^n + \frac{b\varepsilon_0\omega_p^2}{2}M_2\left[\vec{E}^n + \vec{E}^n - \frac{\Delta t}{2\varepsilon_0}\left(\vec{J}^n + \vec{J}^{n+1}\right) + \frac{\Delta t}{\varepsilon_0}\vec{\nabla}\times\vec{H}^{n+1/2}\right]$$

from which an explicit J^{n+1} is obtained:

$$\vec{J}^{n+1} = M_6\vec{J}^n + M_7\vec{E}^n + M_8\vec{\nabla}\times\vec{H}^{n+1/2} \tag{26}$$

where:

$$M_6 = [I + \theta M_2]^{-1}[M_1 - \theta M_2] = \left[I + \theta A^{-1}\right]^{-1}\left[A^{-1}B - \theta A^{-1}\right] \tag{27}$$

$$M_7 = \frac{4\varepsilon_0}{\Delta t}\theta[I + \theta M_2]^{-1}M_2 = 2\frac{\varepsilon_0}{\Delta t}M_8 \tag{28}$$

$$M_8 = 2\theta[I + \theta M_2]^{-1}M_2 = 2\theta\left[I + \theta A^{-1}\right]^{-1}A^{-1} \tag{29}$$

Once J is advanced with (26), E can be advanced with (17), which is simpler than (21).

The above implicit scheme relies on a semi-exponential differencing like the previous explicit scheme. Again, a true exponential differencing can be obtained because of the existence of the analytical solution of the system composed of (6) and the other two components of (1). Unfortunately, like with the explicit scheme, numerical experiments have shown that this true exponential differencing is not stable in some cases.

In summary, by collocating in time the current density with the electric field, implicit advances of E and J are obtained, from which explicit advances can be easily derived by solving a simple local set of two equations. In fact, two implicit schemes have been obtained, the first one composed of (21) for the advance of E and (20) for the advance of J. And the second one composed of (26) for the advance of J and (17) for the advance of E. We denote the two schemes as implicit 1 and implicit 2 (or algorithm 1 and algorithm 2) in the following.

The stability condition of the implicit schemes is the same as in a vacuum (15). This was stated in [9]. We analytically derived the condition in the absence of magnetic field using the same method as for (16) in [6].

4.3. Comparison of the schemes

The major advantage of the implicit schemes is the stability condition (15), which is less severe than (16) and does not depend on the medium. The time step can be larger, which saves computational time, and the height of the computational domain is no longer a critical problem, conversely to the case of the explicit scheme with which the time step strongly depends on the highest electronic density. This renders the implicit schemes highly attractive. Drawbacks are firstly a slightly larger computational time per time step, as can be expected by comparing (5) and (8) with (20) and (21), or with (17) and (26). However, numerical experiments have shown the additional cost per time step is far smaller than the gain resulting from the increase of the time step. Another drawback may be matrices M_3, M_4, M_5 or M_6, M_7, M_8, which depend on the electronic density, conversely to M_1 and M_2. Because they must be computed and stored before the loop on time, this would have been a serious drawback two decades ago [5,6], but nowadays, due to the large memory available on computers, the drawback is minor. In summary, in comparison with the explicit scheme [6], the implicit schemes have a significant advantage, the stability condition (15), and only minor drawbacks.

Let us now compare the two implicit algorithms, relying on (21) and (20), and (26) and (17), respectively. They are not equivalent in terms of computational requirements. Algorithm 2 has several advantages:

- only one equation involves matrices, since there is no matrix in (17). Conversely, both (20) and (21) involve matrices. So that it is expected that the advance of J and E using algorithm 2 can be more rapid;
- algorithm 1 relies on five matrices, M_1, M_2, M_3, M_4, M_5, while algorithm 2 uses only three matrices, M_6, M_7, M_8, and even two in practice, since M_7 and M_8 just differ with the scalar coefficient $\Delta t/2\varepsilon_0$. This has a strong impact on the memory requirements, since the matrices must be computed and stored before the FDTD loop on time. They depend on ω_p and v, so that they must be stored at every FDTD node. Since each matrix has nine entries, with the five matrices of algorithm 1, 45 values must be stored per node. With algorithm 2, the storage is reduced to 18 values.

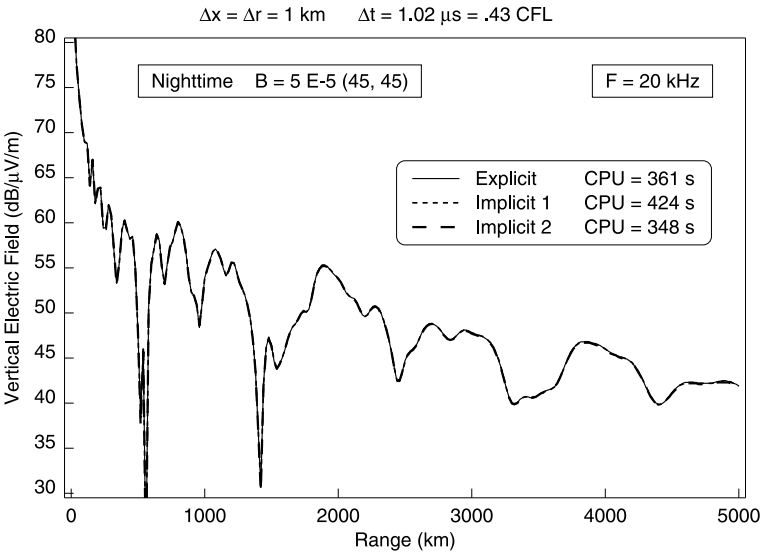

Fig. 3. Comparison of the two implicit schemes with the explicit scheme using the same time step, at frequency 20 kHz.

The two algorithms have been implemented and extensively compared. They yield superimposed results (see next section). The experiments confirmed that algorithm 2 is slightly less demanding in computational time. With, in addition, its dramatic advantage in terms of memory requirements, algorithm 2 is the best one for VLF–LF propagation.

As mentioned in the introduction, an implicit algorithm was presented for the magnetized ionosphere, in [12] and [13]. The formulation in these papers considers the vectors E and J as a whole that form a single vector having six components in the absence of ions, or 12 components when positive and negative ions are present. This algorithm is more costly in terms of computational requirements. For instance, without ions it requires storage of two (6, 6) matrices, that is 72 values at every node of the mesh, in contrast with the 18 values of the scheme (17) and (26). And its computational time is probably significantly larger because the overall number of operations to be performed is far larger. In summary, the algorithm derived in the present paper is more effective than [12,13] in both memory requirements and computational time. Another difference between the two algorithms is the use of a linear differencing in [12] and [13], which renders the algorithm questionable when the condition $\nu\Delta t < 1$ does not hold, as at altitudes 70–80 km in typical VLF–LF radio wave propagation.

5. Numerical experiments

The numerical experiments in this section demonstrate the accuracy of the implicit scheme and illustrate the reduction of CPU time achieved when using it in place of the explicit scheme. In all the computations the transmitter is vertical with power 1 kW, the ground is a PEC, the electronic density (cm^{-3}) and the collision frequency (s^{-1}) are exponential profiles:

$$N(h) = 1.43 \times 10^7 \mathrm{e}^{-0.15h'} \mathrm{e}^{(\beta-0.15)(h-h')} \tag{30}$$

$$\nu(h) = 1.816 \times 10^{11} \mathrm{e}^{-0.15h} \tag{31}$$

where h is the altitude in km, $(\beta,\ h')$ equal (0.5, 87 km) and (0.3, 72 km) for nighttime and daytime, respectively. The natural B field is oriented 45° from the Ground and 45° from the plane of propagation, its magnitude is 0.5 G.

Fig. 3 shows the vertical electric field on the ground, computed with the explicit scheme and the two implicit schemes, at 20 kHz. The vertical and horizontal space steps, Δr and Δx equal 1 km. Δx is defined as $r_{\mathrm{Earth}}\ \Delta\theta$, where $r_{\mathrm{Earth}} =$ 6370 km and $\Delta\theta$ is the FDTD step in θ coordinate. The time step is the same for the three schemes. It equals 90% of the stability limit of the explicit scheme (16), which is about 43% of the CFL condition (15). A very good agreement is observed. The three results differ with less than 0.2 dB on most of the radiopath. Even in the null regions, where the different modes in the waveguide cancel each other, the accordance is good. The computational times (CPU) reported in the figures are similar. As expected, algorithm 2 is slightly more effective than algorithm 1. It is even better than the explicit algorithm (but such comparisons may slightly vary with implementation and some features of the computer). Numerous comparisons were performed with other B field orientations, with daytime profile, and at frequency 60 kHz, in any case the agreement of the different algorithms is quite good.

The major interest of the implicit schemes is the stability condition (15). This is demonstrated in Fig. 4, which is the same as Fig. 3, except that the time steps of the implicit calculations were set to 90% of the CFL condition (15). As can be observed, the CPU time is reduced in proportion to the increase of the time step, i.e. a factor about 2. The accordance of the implicit schemes with the explicit scheme remains good, although less perfect than in Fig. 3. This was expected,

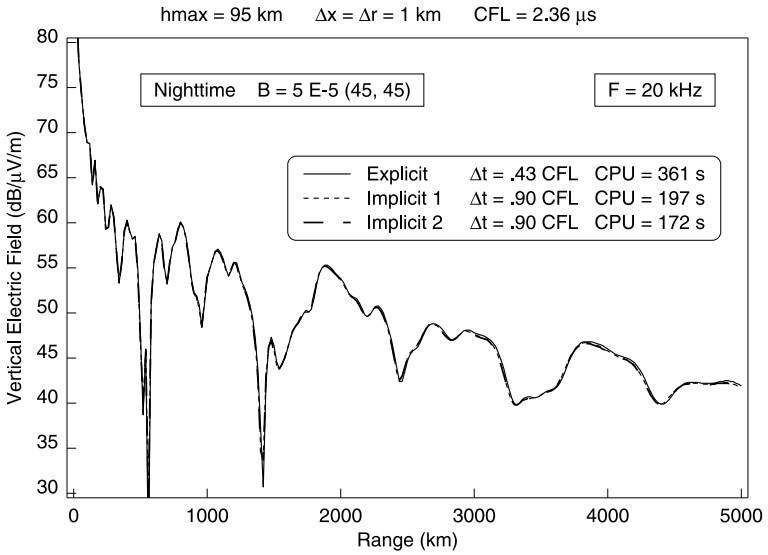

Fig. 4. Comparison of the implicit schemes with the explicit scheme using time steps equal to 90% of the limit of stability for each scheme, at frequency 20 kHz. The top of the domain is at altitude 95 km.

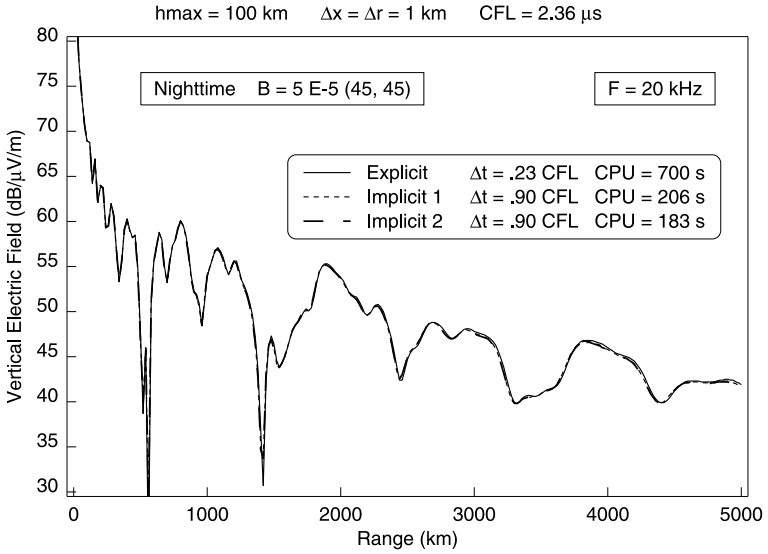

Fig. 5. Comparison of the implicit schemes with the explicit scheme using time steps equal to 90% of the limit of stability for each scheme, at frequency 20 kHz. The top of the domain is at altitude 100 km.

because it is known [8] that the FDTD dispersion depends on the time step. The dispersion is minimum when the step equals the stability limit and increases when it decreases. In facts, the results with the implicit schemes and the largest step are probably better than the explicit results, because of lesser numerical dispersion.

Fig. 5 is like Fig. 4, except that the altitude of the top of the computational domain was 100 km in place of 95 km. The maximum electronic density is higher, so that the explicit limit of stability (16) is reduced. From this, the time step of the explicit calculation was reduced from 0.43 CFL to 0.23 CFL and then the computational time was doubled. Conversely, with the implicit schemes, the time step can be left unchanged so that the increase of CPU time is only due to the additional 5-km space. The net result is a ratio of 4 between the CPU times of the explicit and implicit schemes. This example clearly demonstrates the interest of explicit schemes. They render the computational time relatively insensitive to the altitude of the top of the domain. Since the altitude of reflection of the VLF–LF waves is only approximately known, with the implicit scheme a margin can be added to the altitude of the top, without significant increase in the CPU time.

Fig. 6 shows results at 60 kHz, with the top at 100 km. The reduction of the CPU time is smaller than at 20 kHz. This is because the physics of the medium is the same, but the space steps are smaller, so that the explicit stability condition (16) is closer to the stability in a vacuum. From this, the gain from using the implicit schemes is smaller.

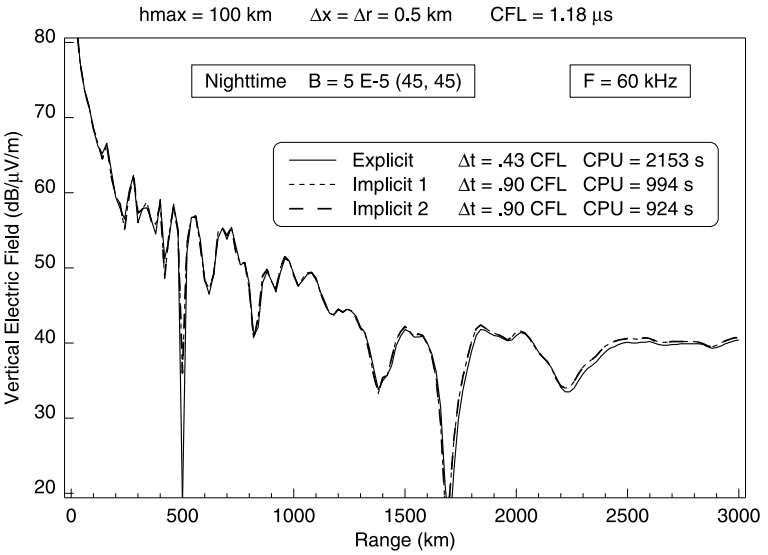

Fig. 6. Comparison of the implicit schemes with the explicit scheme using time steps equal to 90% of the limit of stability for each scheme, at frequency 60 kHz. The top of the domain is at altitude 100 km.

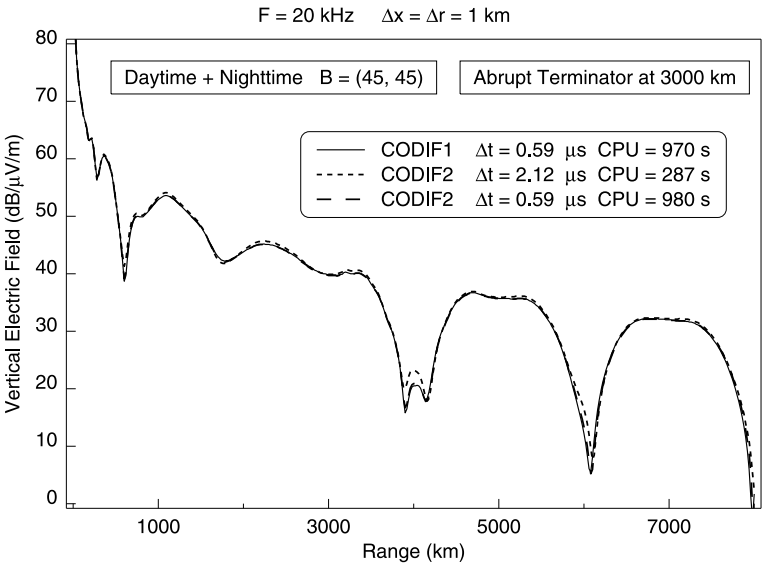

Fig. 7. Comparison of the computer codes CODIF1 (explicit scheme) and CODIF2 (implicit 2 scheme) with a daytime–nighttime terminator. With CODIF2 one calculation was performed with CODIF1 time step [90% of (16)] and one calculation with its own step [90% of (15)].

Fig. 7 is another comparison with a radiopath in part in daytime and in part in nighttime. The results are denoted as CODIF1 and CODIF2 which are two versions of the computer code CODIF, relying on the explicit scheme and the implicit scheme (algorithm 2), respectively. Again, the results are in good accordance, with a large reduction of the computational time with CODIF2 when using the large time step allowed by (15). The top of the domain was at 99 km on the whole path with the implicit scheme, while with the explicit one it was at 99 km in nighttime, but only at 83 km in daytime, not to have a too severe constraint (16). This illustrates another advantage of the implicit scheme. In inhomogeneous radiopaths, there is no need of varying the top of the domain in function of the local electronic profile.

6. Conclusion

The FDTD calculation of VLF–LF propagation in the Earth–ionosphere waveguide is significantly improved by using the new implicit scheme in place of the explicit scheme [6]. The improvement results from the stability condition which is less severe and does not depend on the physical parameters of the ionosphere. This permits the computational time to be

reduced significantly, and this renders the computations easier and more reliable because a margin can be added to the height of the computational domain without significant penalty in terms of computational time.

The VLF–LF computer code relying on the FDTD method is a tool that can be used to perform extensive computations. Its computational time is now relatively small, even on a personal computer (PC). For example, for an 8000-km radiopath at frequency 20 kHz, and a good accuracy of the calculation (accuracy 4 on a scale of 5, see details in [7]), the CPU time is smaller than 1 min on a 3-GHz PC. At 60 kHz, it is about 10 min for a 5000-km radiopath. These CPU times can be easily reduced further by using Open MP parallelization, which permits to take advantage of the multi-thread possibilities of PCs. With an 8-thread PC, typical CPU times are then 10 s at 20 kHz and 1–2 min at 60 kHz.

References

[1] K. Davies, Ionospheric Radio, IEE Electromagn. Waves Ser., London, 1990.
[2] F.J. Kelly, ELF/VLF/LF propagation and system design, Report 9028, Naval Research Laboratory, Washington DC, 1987.
[3] D.F. Morfitt, R.F. Halley, Comparison of waveguide and wave hop techniques for VLF propagation modeling, Naval Weapons Center, China Lake, CA, 1970, NWC Techniques Publication 4952.
[4] J.-P. Bérenger, FDTD Computation of VLF–LF propagation in the Earth–ionosphere waveguide, in: EUROEM94 Symp, Bordeaux, France, June 1994.
[5] M. Thévenot, J.-P. Bérenger, T. Monedière, F. Jecko, A FDTD scheme for the computation of VLF–LF propagation in the Anisotropic Earth–Ionosphere Waveguide, URSI Gen. Ass., Lille, France, September 1996.
[6] M. Thévenot, J.-P. Bérenger, T. Monedière, F. Jecko, A FDTD scheme for the computation of VLF–LF propagation in the anisotropic Earth–ionosphere waveguide, Ann. Telecommun. 54 (1999) 297–310.
[7] J.-P. Bérenger, FDTD computation of VLF–LF propagation in the Earth–ionosphere waveguide, Ann. Telecommun. 57 (2002) 1059–1090.
[8] A. Taflove, S.C. Hagness, Computational Electrodynamics: The Finite-Difference Time-Domain Method, Artech House, 2005.
[9] S.A. Cummer, An analysis of new and existing FDTD methods for isotropic cold plasma and a method for improving their accuracy, IEEE Trans. Antennas Propag. 45 (1997) 392–400.
[10] J.H. Lee, D.K. Kalluri, Three-dimensional FDTD simulation of electromagnetic wave transformation in a dynamic inhomogeneous magnetized plasma, IEEE Trans. Antennas Propag. 47 (1999) 1146–1151.
[11] S.A. Cummer, Modeling electromagnetic propagation in the Earth–ionosphere waveguide, IEEE Trans. Antennas Propag. 48 (2000) 1420–1429.
[12] W.H. Hu, S.A. Cummer, An FDTD model for low and high altitude lightning-generated EM fields, IEEE Trans. Antennas Propag. 54 (2006) 1513–1522.
[13] Y. Yu, J. Simpson, An $E-J$ collocated 3-D FDTD model of electromagnetic wave propagation in magnetized cold plasma, IEEE Trans. Antennas Propag. 58 (2010) 469–479.